Stochastic Simulation of Land-Cover Change Using Geostatistics and Generalized Additive Models

Daniel G. Brown, Pierre Goovaerts, Amy Burnicki, and Meng-Ying Li

Abstract

An approach to simulating land-cover change based on pairs of classified images is presented. The method conditions the simulations on three sources of information: an initial land-cover map, maps of the probabilities of each possible class transition, and a description of the spatial patterns of changes (e.g., semivariograms). The method can produce multiple simulated land-cover maps that honor each of these sources of information. The approach is demonstrated for data on forest-cover change near Traverse City, Michigan. The discussion describes extensions to the method and an approach to generating future land-cover scenarios based on socioeconomic information.

Introduction

Land-cover change has caused and will continue to cause dramatic changes in the structure and function of ecosystems (Meyer and Turner, 1994). Projections of future land-cover patterns are needed to evaluate the implications of human action for the future of ecosystems (Turner *et al.*, 1995). Models that predict future land-cover patterns can support generation of plausible scenarios for assessing land-cover conditions under a range of assumptions about rates and patterns of change that reflect current and recent trends.

Although much work is needed to add more realistic representations of human decision making in models of land-use and land-cover change (Bockstael, 1996; Polhill *et al.*, 2001), models that simply project current trends into the future have some value in land-cover scenario development, but are not yet fully developed. Models that project current and recent trends, and present a range of outcomes that reflect these trends, can serve as useful benchmarks, if nothing else, against which more process-oriented models can be compared. To be useful, however, projective models need to represent, with reference to current and recent trends, the (1) amounts of land-cover changes, (2) locations of future changes, and (3) spatial patterns of those changes. Although several models exist to address the first two of these conditions (Veldkamp and Fresco, 1996; Landis and Zhang, 1998; Pijanowski *et al.*, in press), few models exist that specifically aim to reproduce the spatial patterns of land-cover changes. Predicted spatial patterns resulting from models that do not seek to specifically reproduce spatial patterns of change are often artifacts of the patterns in input variables. Representing spatial patterns of change is important because it is the only way to evaluate the consequences of current and recent land-cover trends for the future fragmentation of the landscape.

Transition probability models have been used extensively for analysis and stochastic modeling of land-use and land-cover change (Bell, 1974; Turner, 1987; Muller and Middleton, 1994). Increasingly, these models use spatially variable transition probabilities to account for the effects of exogenous variables on the transition process (Baker, 1989; Brown *et al.*, 2000b). To estimate probabilities of land-use transition, land-use change is typically modeled as a function of variables describing (1) biophysical land quality (e.g., soils and terrain) and (2) location relative to jobs, markets, and amenities (Landis and Zhang, 1996; Pijanowski *et al.*, in press). These models are usually calibrated using maps of observed change. Modelers have used linear statistical models, such as logistic regression (Wear *et al.*, 1998; Schneider and Pontius, 2001) and non-linear approaches, like artificial neural networks (Pijanowski *et al.*, in press), because the relationships between the predictor variables and land-use change are not always linear. Generalized additive models (GAMs) offer a non-linear statistical alternative to logistic regression (Hastie and Tibshirani, 1990). For example, Brown (1994) implemented GAMs for the estimation of land-cover patterns in Glacier National Park and found significant non-linear relationships with topographic and disturbance variables.

Spatial description and simulation of spatial patterns is a mainstay of geostatistics (Goovaerts, 1997), which provides a set of statistical tools to analyze and predict variables that vary in time and space. Indicator semivariograms allow one to characterize the spatial patterns of categorical variables, while indicator cross semivariograms provide information on the frequency of transitions between different categories (Carle and Fogg, 1996; Carle and Fogg, 1997). Goovaerts (1997) and de Bruin (2000) used categorical indicator semivariograms to characterize the spatial distribution of land covers. Another application of geostatistics is the simulation of patterns that honor observations at data locations and reproduce global spatial information (histogram, covariance function, or semivariogram) as inferred from the data (Kyriakidis and Dungan, 2001). Multiple equally probable maps can be generated then fed into GIS operators (e.g., classification), allowing one to assess how the uncertainty about the spatial distribution of environmental attributes translates into uncertainty about classification

D.G. Brown and A. Burnicki are with the Environmental Spatial Analysis Lab, School of Natural Resources & Environment, University of Michigan, Ann Arbor, MI 48109-1115 (danbrown@umich.edu).

P. Goovaerts and M-Y. Li are with the Department of Civil & Environmental Engineering, University of Michigan, Ann Arbor, MI 48109 (goovaert@umich.edu).

Photogrammetric Engineering & Remote Sensing
Vol. 68, No. 10, October 2002, pp. 1051–1061.

0099-1112/02/6810–1051$3.00/0

results (Burrough and McDonnell, 1997; Moeur and Riemann-Hershey, 1999; De Bruin, 2000).

We present a geostatistical simulation approach to generating multiple possible realizations of future forest cover based on an initial map, a description of the spatial patterns of change, and maps of land-cover transition probabilities. The spatial patterns of the land-cover transition probabilities were predicted using spatial and ecological variables and generalized additive models (GAMs) that were calibrated to a two-date time series of land-cover data. To illustrate the method, we focus on clearing and regrowth of forests in a study area in northern Lower Michigan.

Pilot Data Set

After describing the methodology, we illustrate the approach by projecting forest cover change for a pilot study area in which we have collected and classified time series Landsat Multispectral Scanner (MSS) imagery and a GIS database. The approx. 5000 ha (18 survey sections) area lies immediately adjacent to the south and east of Traverse City, Michigan, a town of about 15,000 residents that serves as a market center for a region distinguished by natural amenities (i.e., lakes, forests, and Great Lakes shoreline) and an economy based increasingly on recreation and natural amenities (Figure 1). North American Landscape Characterization (NALC) data were acquired and processed as part of a larger project to characterize land-use and land-cover change across the Upper Midwest (Brown *et al.*, 2000a). The NALC project compiled and georeferenced three dates of MSS images for all of the United States and Canada (Lunetta *et al.*, 1998). The dates acquired for the study site, which falls in WRS path 22 and row 29, were 10 June 1973, 28 June 1985, and 15 July 1991. They were each classified to four different land-cover classes: forest, nonforest, water, and missing (i.e., clouds and cloud shadows). The classification accuracies (percent correctly classified) for the three dates are 76.8, 85.6, and 79.2, respectively, based on random sample points taken from one half of the site and compared to classifications made through interpretation of aerial photography. Though we do not have an estimate of positional uncertainty, the spatial registration of the data sets was evaluated through overlay. As a result, the 1985 image location was adjusted to match that of the 1973 image. Our demonstration of the method in this paper uses only the 1973 (time t_1) and 1985 (time t_2) images (Figures 2a and 2b) and only two land covers: forest (F = s_1) and nonforest (NF = s_2), leading to two types of indicators of transition: $i(\mathbf{u}, t_2 - t_1; s_1, s_2)$ and $i(\mathbf{u}, t_2 - t_1; s_2, s_1)$, where $\mathbf{u}$ is a vector of spatial coordinates. The observed transitions are shown in Figure 2c.

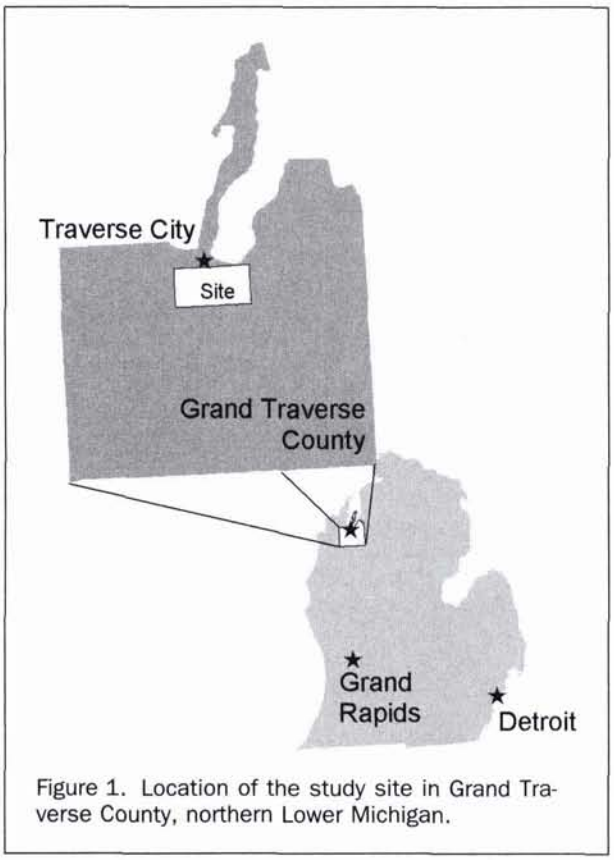

Figure 1. Location of the study site in Grand Traverse County, northern Lower Michigan.

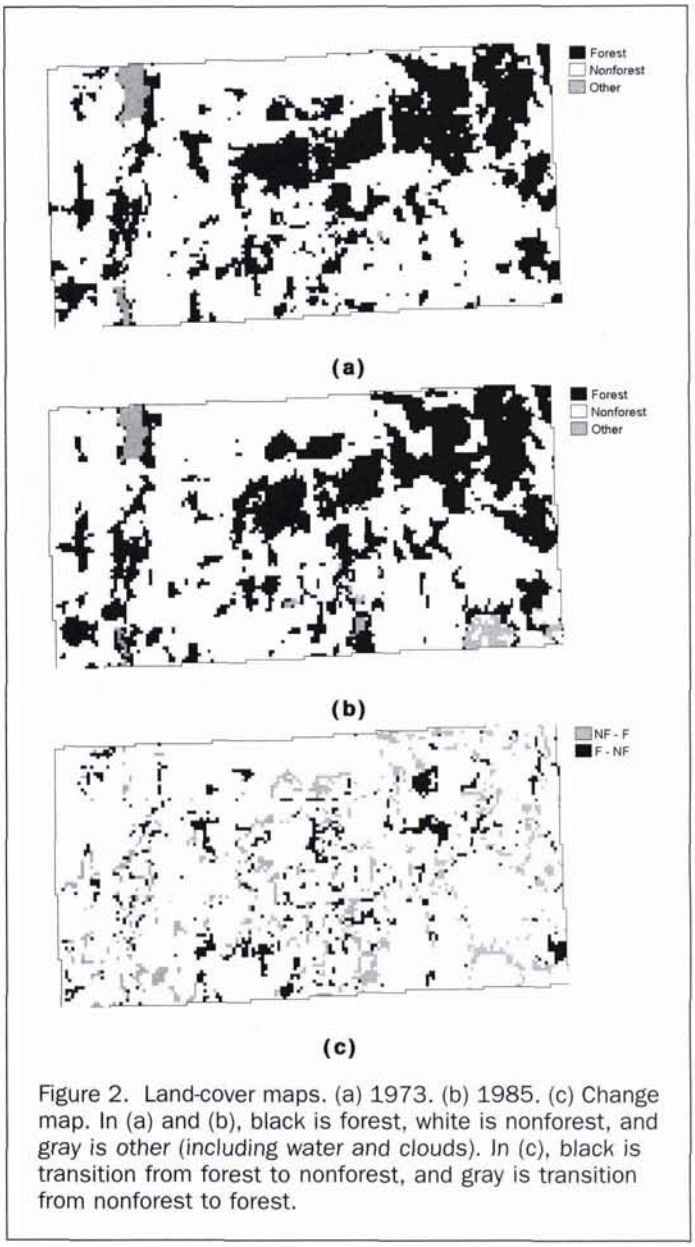

Figure 2. Land-cover maps. (a) 1973. (b) 1985. (c) Change map. In (a) and (b), black is forest, white is nonforest, and gray is other (including water and clouds). In (c), black is transition from forest to nonforest, and gray is transition from nonforest to forest.

Methods

The method of generating future land-cover maps presented here uses a geostatistical simulation algorithm that is conditioned on an initial land-cover map, a map of transition probabilities, and geostatistical descriptions of the patterns of change. For our illustration we base the transition probability map and geostatistical descriptions of change on the observed

patterns of change (Figure 2c). The transition probability map is created using one third of the observed transitions in the study site to fit a generalized additive model, which is then used to estimate transition probabilities for all cells. Because the simulation approach is stochastic, multiple realizations of the future land-cover map can be generated to provide spatial information about the likelihood of change. We describe the approach to estimating transition probabilities using generalized additive models, the use of semivariograms and cross semivariograms to describe the patterns of change, and the simulation algorithm, and apply the approach in an illustration.

Predicting Transition Probabilities

Let $\{s_k; k = 1, \ldots, K\}$ be a set of K mutually exclusive land covers (LC) observed over the study area. The LC recorded at location $\mathbf{u}$ and time t_1 is denoted $s(\mathbf{u}, t_1)$, and the difference between LC observed at two times t_1 and t_2 can be coded using the following indicator variable:

$$i(\mathbf{u}, t_2 - t_1; s_k, s_{k'}) = 1 \text{ if } s(\mathbf{u}, t_1) = s_k \text{ and } s(\mathbf{u}, t_2) = s_{k'}; \quad (1)$$
$$= 0 \text{ otherwise.}$$

Because locations on the map vary in the propensity to transition, the simulation requires, first, estimation of the spatial distribution of transition probabilities (i.e., the probability that $i(\mathbf{u}, t_2 - t_1; s_k, s_{k'})$ is equal to 1). The goal of the estimation is to produce a vector of probabilities $p(\mathbf{u}_j, \Delta t; s_k, s_{k'})$ for all locations $j = 1, \ldots, N$ and all pairs of classes $s_k, s_{k'}$. Models of transition probabilities were based on several exogenous variables fit using generalized additive modeling (GAM).

Logistic regression takes the form

$$g(\mu) = a + \sum_{j=1}^{p} (\beta_j x_j) \quad (2)$$

where $g(\mu)$ is the the linear predictor, a is the intercept, β_j is the coefficient estimate for jth variable, x_j is the value for the jth variable, and p is the number of predictor variables. The linear predictor $[g(\mu)]$ is related to the probability of occurrence through the logit link function, which calculates the probability that the modeled category occurred using

$$p(y) = \frac{e^{g(\mu)}}{1 + e^{g(\mu)}} \quad (3)$$

where $p(y)$ is the probability that y [i.e., $i(\mathbf{u}, t_2 - t_1; s_k, s_{k'}]$ is 1.

GAMs relax the assumption of logistic regression, that the predictor variables (the x_js) are related to the dependent variable in a log-linear way. The non-parametric logistic regression equation, under the relaxed assumption, becomes

$$g(\mu) = a + \sum_{j=1}^{p} f_j(x_j) \quad (4)$$

where f_j are unspecified smoothed functions for each of the predictor variables. The functions can be estimated through a variety of smoothing techniques (Hastie and Tibshirani, 1990); here we use spline smoothing. The f_js can be plotted as functions of the values of each variable (j).

We fit a separate model for each type of transition between forest and nonforest (i.e., from F to NF and from NF to F). Variables that were tested for inclusion in the models to predict transition probabilities are listed in Table 1. These variables were hypothesized to affect either the value of the land in terms of access to population centers and relative to markets (i.e., the situation) or the inherent biophysical properties of the land that affect its value and the tree growth rates (i.e., the site). All variables were constructed using GIS analysis functions provided within the IDRISI software package (Clarklabs, Worcester, Massachusetts). All distance variables, slope, and curvature were computed using the corresponding IDRISI modules. Aspect relative to south was calculated as the cosine of the difference between cell aspect and 180 degrees (i.e., south). The topographic wetness index was the same as that used by Phillips (1990) and is the natural log of the number of cells flowing into a cell divided by the slope of the cell. All variable maps were aggregated from the 30-m resolution of the digital elevation model to match the 60-m resolution of the NALC data by averaging cell values after the variables had been computed.

The pilot landscape was sampled systematically by taking every third 60- by 60-m cell on every third line. This was to reduce the effects of spatial autocorrelation, though it was still present in the sample. At present, no form of GAM allows the incorporation of spatial dependence into the estimation of the model parameters. However, we do include spatial variables that should account for spatial dependence in the transition processes. In the case of NF to F the sample resulted in 120 transitioning cells and 894 non-transitioning cells; for F to NF we had 104 transitioning and 1301 non-transitioning cells.

The GAMs were fitted using a forward stepwise procedure in which the variable that contributed the most to reducing the residual deviance in the model was added at each step. As each variable was added to the model, the degree to which the variable had a non-linear relationship with the transition occurrence was tested using chi-square statistics. Where relationships were not significantly different from linear, a linear fit was used. For non-linear relationships the function was fitted with a spline smoothed function. Fitted relationships for linear and non-linear variables are reported as graphs of the linear predictor versus variable values.

The overall fit of the models was measured using a summary of the deviance explained by the model [i.e., (null deviance − residual deviance)/null deviance]. The derived value is termed D^2 and is analogous, though not identical, to an R^2 in ordinary least-squares regression. The predictive power of each model at each step was measured by classifying estimated probability values. Crosstabulation of predicted and observed occurrences of change resulted in two additional statistics describing the fit of the models: the percent of observations correctly classified (PCC) by the model and the odds ratio, which is the product of the numbers of correctly classified cells (i.e., number of correctly classified forest cells times the number of correctly classified nonforest cells) divided by the product of the numbers of incorrectly classified cells. PCC varies in the range [0,1], with one indicating perfect prediction of the occurrence of transitions. The odds ratio is a dimensionless measure in the range $[0,\infty]$ that provides an alternative indicator of the ability of the model to predict the observations to which it was fitted. In order to compute the PCC and odds ratio, a threshold probability was selected to assign predicted transitions, such that the predicted number of transitions was equal to the observed number of transitions.

The GAM models of NF to F and F to NF transition probabilities, fitted with one-third of the cells using the method described above, were used to estimate the transition probability of every cell in the pilot study site. Because non-linear functions in GAMs are estimated for each value of the predictor variables that are presented to the model, some interpolation and/or extrapolation of transition probability estimates is required whenever the locations to be estimated have values for predictor variables that were not used in model calibration. These interpolations and extrapolations are based on the spline functions fitted to the models. We used S-Plus (MathSoft, Inc., Seattle, Washington) both to fit the models to the sample data set and to apply the models for

TABLE 1. VARIABLES TESTED FOR INCLUSION IN THE GENERALIZED ADDITIVE MODEL (GAM) OF TRANSITION PROBABILITIES

Access Variables	Units	Abbr.	Source
Distance to Nearest Highway	m	DHI	digitized 1:24,000 topographic maps
Distance to Nearest Major Road	m	DMR	digitized 1:24,000 topographic maps
Distance to Nearest Residential Streets	m	DRS	digitized 1:24,000 topographic maps
Distance to Traverse City	m	DTC	USGS GNIS
Water Features			
Distance to Nearest Inland Lake	m	DIL	digitized 1:24,000 topographic maps
Distance to Bay Shore	m	DBS	digitized 1:24,000 topographic maps
Distance to Nearest Perennial Streams	m	DPS	digitized 1:24,000 topographic maps
Site Attributes			
Elevation	m	ELE	USGS 7.5 minute DEM (30 m)
Slope	°	SLO	from USGS 7.5 minute DEM
Plan Curvature	None	CUR	from USGS 7.5 minute DEM
Aspect relative to South	cos(°)	ASP	from USGS 7.5 minute DEM
Topographic wetness index	none	TWI	from USGS 7.5 minute DEM
Initial Map			
Distance to Forest	m	DFO	derived from classified MSS image
Distance to Not Forest	m	DNF	derived from classified MSS image
Num of Forest Neighbors (5×5 window)	count	NFO	derived from classified MSS image
Num of Not Forest Neighbors (5×5 win)	count	NNF	derived from classified MSS image

estimating the transition probabilities at all cells. The resulting maps were then used for simulation.

Geostatistical Model of Change

Landscape changes do not usually occur randomly in space; that is, neighboring pixels $\mathbf{u}$ and $\mathbf{u}'$ are more likely to undergo similar changes, which means that $i(\mathbf{u}', t_2 - t_1; s_k, s_{k'})$ tends to equal $i(\mathbf{u}, t_2 - t_1; s_k, s_{k'})$ for all $s_k, s_{k'}$. Spatial patterns of temporal changes can be characterized using geostatistical tools such as the semivariogram (Goovaerts, 1997) that is estimated as

$$\hat{\gamma}(\mathbf{h}, t_2 - t_1; s_k, s_{k'}) = \frac{1}{2N(\mathbf{h})} \sum_{\alpha=1}^{N(\mathbf{h})} [i(\mathbf{u}_\alpha, t_2 - t_1; s_k, s_{k'}) - i(\mathbf{u}_\alpha + \mathbf{h}, t_2 - t_1; s_k, s_{k'})]^2 \quad (5)$$

where $N(\mathbf{h})$ is the number of data pairs (e.g., pairs of pixels) separated by a vector $\mathbf{h}$. The indicator semivariogram can be interpreted as half the frequency of transition from one type of temporal change (i.e., s_k at t_1 to $s_{k'}$ at t_2) to any other type over a separation vector $\mathbf{h}$. It is thus a measure of the lack of spatial connectivity of temporal changes: the smaller the value of the semivariogram (Equation 2), the higher the connectivity. Note that this frequency of transition is averaged over all locations $\mathbf{u}_\alpha$ to become solely a function of the separation vector $\mathbf{h}$, which corresponds to an assumption of stationarity or homogeneity of the spatial domain. Similarly, an assumption of stationarity over the temporal domain would allow the frequency to become a function of the time interval Δt: i.e.,

$$\hat{\gamma}(\mathbf{h}, \Delta t; s_k, s_{k'}) = \frac{1}{2N(\mathbf{h})} \sum_{\alpha=1}^{N(\mathbf{h})} [i(\mathbf{u}_\alpha, \Delta t; s_k, s_{k'}) - i(\mathbf{u}_\alpha + \mathbf{h}, \Delta t; s_k, s_{k'})]^2. \quad (6)$$

Experimental semivariograms are computed along different directions; then permissible models (e.g., spherical, exponential) are fitted to experimental curves so that frequencies of transitions can be retrieved for any possible combination of distance and direction.

Besides the semivariograms of the two types of change (F to NF and NF to F), the cross semivariogram between the indicators of the two types of changes can be computed as

$$\hat{\gamma}(\mathbf{h}, \Delta t; s_k, s_{k'}; s_{k'}, s_k) = \frac{1}{2N(\mathbf{h})} \sum_{\alpha=1}^{N(\mathbf{h})} [i(\mathbf{u}_\alpha, \Delta t; s_k, s_{k'}) - i(\mathbf{u}_\alpha + \mathbf{h}, \Delta t; s_k, s_{k'})] \times [i(\mathbf{u}_\alpha, \Delta t; s_{k'}, s_k) - i(\mathbf{u}_\alpha + \mathbf{h}, \Delta t; s_{k'}, s_k)]. \quad (7)$$

The cross semivariogram describes the frequency with which two pixels separated by a vector $\mathbf{h}$ will jointly change land cover in opposite ways: one will go from F to NF, while the other one will change from NF to F. By construction, the cross semivariogram takes only negative values because these changes are mutually exclusive.

Simulation

Let $\{s(\mathbf{u}_j, t), j = 1, ..., N\}$ be the LC recorded at time t over N grid nodes or pixels $\mathbf{u}_j$ discretizing the study area A. The objective is to predict the spatial distribution of LC at time $t + \Delta t$, accounting for the set of transition probabilities $\{p(\mathbf{u}_j, \Delta t; s_k, s_{k'}), j = 1, \ldots, N\}$ and the (cross)semivariogram models fitted to the curves of Equations 6 and 7. Given the current LC at $\mathbf{u}_j$, the probability of occurrence of any LC $s_{k'}$ at time $t + \Delta t$ is easily computed as

$$p(\mathbf{u}_j, t + \Delta t; s_{k'}) = \sum_{k=1}^{K} p(\mathbf{u}_j, \Delta t; s_k, s_{k'}) \times i(\mathbf{u}_j, t; s_k) \quad (8)$$

where the indicator variable $i(\mathbf{u}_j, t; s_k) = 1$ if LC s_k is recorded at time t, and zero otherwise.

There are different ways to account for the vector of local probabilities of occurrence $[p(\mathbf{u}_j, t + \Delta t; s_k), k = 1, ..., K]$ when predicting land cover. For example, a 0.1 probability $p(\mathbf{u}_1, t + \Delta t; s_1)$ means that node $\mathbf{u}_1$ has one chance in ten to be under forest. Another way of interpreting such probabilities is that, out of ten nodes with a 0.1 probability, one node should be under forest. Following an approach developed by Goovaerts and Journel (1996), all N nodes are categorized into L classes of probability of transition and within each class a proportion of nodes, referred to as "local class proportions" and denoted p_{kl}, are forced to change class.

Simulated annealing is used to generate land-cover maps that reproduce both target local class proportions and (cross)-semivariograms of changes. The idea is to gradually perturb the

LC map at time t so as to minimize an objective function that measures the deviation between target and current statistics of the LC map. The objective function $O = \omega_1 O_1 + \omega_2 O_2$, with $\omega_1 + \omega_2 = 1$, includes two components: local class proportions and (cross) semivariogram models over the first J lags $\mathbf{h}_j$: i.e.,

$$O_1 = \sum_{k=1}^{K} \sum_{l=1}^{L} [p_{kl} - p_{kl}^*]^2 \quad (9)$$

$$O_2 = \sum_{j=1}^{J} \left(\sum_{k=1}^{2} \sum_{k' \neq k} [\gamma(\mathbf{h}_j, \Delta t; s_k, s_{k'}) - \gamma^*(\mathbf{h}_j, \Delta t; s_k, s_{k'})]^2 + [\gamma(\mathbf{h}_j, \Delta t; s_k, s_{k'}; s_{k'}, s_k) - \gamma^*(\mathbf{h}_j, \Delta t; s_k, s_{k'}; s_{k'}, s_k)]^2 \right) \quad (10)$$

where p_{kl}^* and $\gamma^*(\mathbf{h}_j, \Delta t; s_k, s_{k'})$ are the current local class proportion and value of the semivariogram of the simulated image, respectively. To prevent the component with the largest unit to dominate the objective function, the first component is standardized by its initial value, while the semivariogram models are standardized by their sills.

The objective function is lowered using a variant of simulated annealing, called the MAP (maximum *a posteriori*) algorithm (Winkler, 1995) that proceeds as follows:

(1) Compute the value of the objective function for the initial image.
(2) For a specified number of iterations, define a random path that visits all non-conditioned grid nodes; at each node $\mathbf{u}_j$ consider the two possible LCs and compute the corresponding objective function values; select the LC (F or NF) associated with the smallest objective function value; and proceed to the next node along the random path.

The process is stopped when the percentage of changes from iteration $i-1$ to iteration i decreases below a given threshold value. Other realizations are generated by repeating the procedure using other random paths.

Evaluation

To illustrate the method, we estimate transition probabilities and patterns of change from the 1973 to 1985 change data. The simplest version of the method was used for illustration purposes. Simulations of the 1985 map were created using the 1973 initial map and compared with the observed map to validate the methodology. Because the model was calibrated based on the observed change from 1973 to 1985, we were simply testing how well the simulations reproduce that map. First, we compared the forest and nonforest proportions in the realizations versus the actual 1985 proportions. Then, reproduction of transition probabilities was quantified by computing, for each pixel, the proportion of times it changes LC class over 100 realizations and comparing the simulated probabilities with the target values. The rank correlation between simulated and target transition probabilities was then computed. To assess the reproduction of spatial patterns of changes, direct and cross indicator semivariogram values computed from the first simulated LC map were overlaid on target models.

Results

Spatial Transition Probability Models

The final model of probabilities for the NF to F transition reduced the deviance (the measure of variation used in GAMs) by 25 percent (Table 2). The threshold value used for assigning probabilities to transitions and evaluating model predictions was 0.293. The resulting assignment correctly predicted 87 percent of the transition and non-transition cells, with odds-ratio of 10.26. The F to NF transition model exhibited a 24 percent reduction in deviance (Table 2). With a prediction threshold

TABLE 2. FINAL MODEL FITS AND TESTS FOR VARIABLE NON-LINEARITY (SHOWN ONLY FOR THOSE INCLUDED AS NON-LINEAR) FROM GAM ANALYSIS

	N	Null Deviance	Residual Deviance	D2	Odds Ratio	PCC	ChiSq	P(chi)
NF to F	1014	737.403	554.476	0.25	10.26	0.87		
DMR							—	—
DRS							10.30	0.01
DHI							8.95	0.03
NFO							—	—
DFO							—	—
F to NF	1405	741.612	560.838	0.24	7.59	0.90		
NNF							62.76	<0.01
DIL							16.59	<0.01
DTC							12.04	0.01
DHI							—	—
DMR							—	—

value of 0.241, the model correctly predicted 90 percent of the transition and non-transition cells and had an odds-ratio of 7.59. Five variables were included in each of the final models for NF to F and F to NF transitions, and the chi-square test for non-linearity is listed for those that exhibited a significant degree of non-linearity (Table 2). Plots of the relationships and partial residuals for each of the predictor variables reveal the nature and shape of the functions (Figures 3 and 4). For variables in which the relationships were not significantly different from log-linear, the fitted line (solid) is straight. For all others, the shape of the solid line describes the non-linear nature of the relationship. Many more of the partial residuals are below the solid line than above because there are more cells that do not transition in our sample than do.

Transitions from NF to F were more likely in non-forested cells that were nearer to forested cells and/or with more forest cells in the 5 by 5 window around the cell (Figure 3a and 3e). These variables (i.e., NFO and DFO) were both linearly related to the probability of NF to F transition and suggested a strong spatial interaction, such that regrowth and/or planting of trees was more likely near existing forest patches. The other three variables that were added to the model represented the distance from the cell to each of three classes of roads. A linear relationship was observed between the probability of transition and the distance to major roads, such that regrowth and/or planting was more likely with increasing distance from major roads (Figure 3b). A similar, but non-linear, relationship was observed with distance to residential streets (Figure 3c). The relationship is non-linear because the distance effect levels off beyond about 400 meters, such that the NF to F transition is less likely closer to residential streets within 300 to 400 meters but there is no relationship after 400 meters. Distance to highways exhibits a relationship that levels off with distance as well, but the nature of the relationship is reversed (Figure 3d). The NF to F transition is more likely close to major highways up to a distance of about 1000 meters.

The probability of forest clearing (F to NF) tended to be highest where there was a moderate number (four to seven) of nonforested cells in the 5 by 5 neighborhood of a forested cell (Figure 4a). This suggests that the cells most likely to be cleared are not parts of single isolated patches of one or a few cells, but rather more likely to be on concave edges of larger patches. Cells towards the interior of larger patches tend not to be cleared. The F to NF transition probability tended to decrease with increasing proximity to inland lakes (Figure 4b), though this was a local effect with no relationship observed beyond about 2 km. Probability of clearing decreased with increasing distance from Traverse City, though there was a slight increase in probability between about 6 and 7 km from the city (Figure

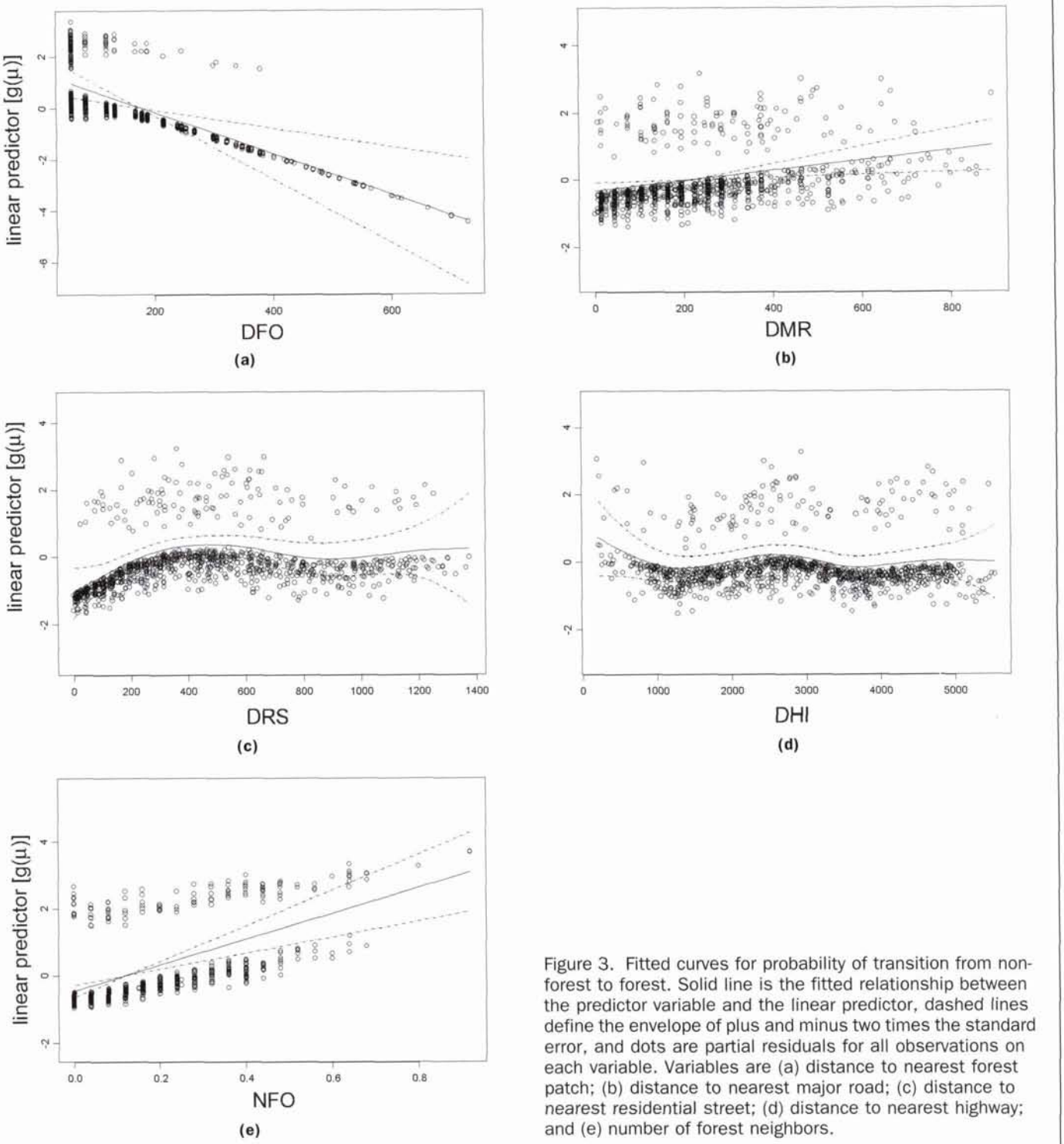

Figure 3. Fitted curves for probability of transition from nonforest to forest. Solid line is the fitted relationship between the predictor variable and the linear predictor, dashed lines define the envelope of plus and minus two times the standard error, and dots are partial residuals for all observations on each variable. Variables are (a) distance to nearest forest patch; (b) distance to nearest major road; (c) distance to nearest residential street; (d) distance to nearest highway; and (e) number of forest neighbors.

4c), perhaps indicating a zone of active peri-urban development. As a complement to the NF to F transition model, the F to NF transition probability increases with distance from highways (Figure 4d). Similarly, clearing was somewhat more likely on cells that were nearer to major roads (Figure 4e).

Spatial patterns in the transition probability maps [$p(\mathbf{u}_j, \Delta t; s_k, s_{k'})$] for the NF to F and F to NF transitions (Figures 5a and 5b, respectively) reflect the patterns of variables used in the model. Although a value is assigned to every cell in Figures 5a and 5b, the models were fitted and values used only for those cells that have the initial class of the transition. For example, though forested cells in 1973 have a transition probability for NF to F, they cannot undergo that transition because they do not have the nonforest label initially.

Descriptions of Spatial Patterns of Change

Direct and cross semivariograms of indicators of changes F to NF and NF to F were computed along the north-south and east-west

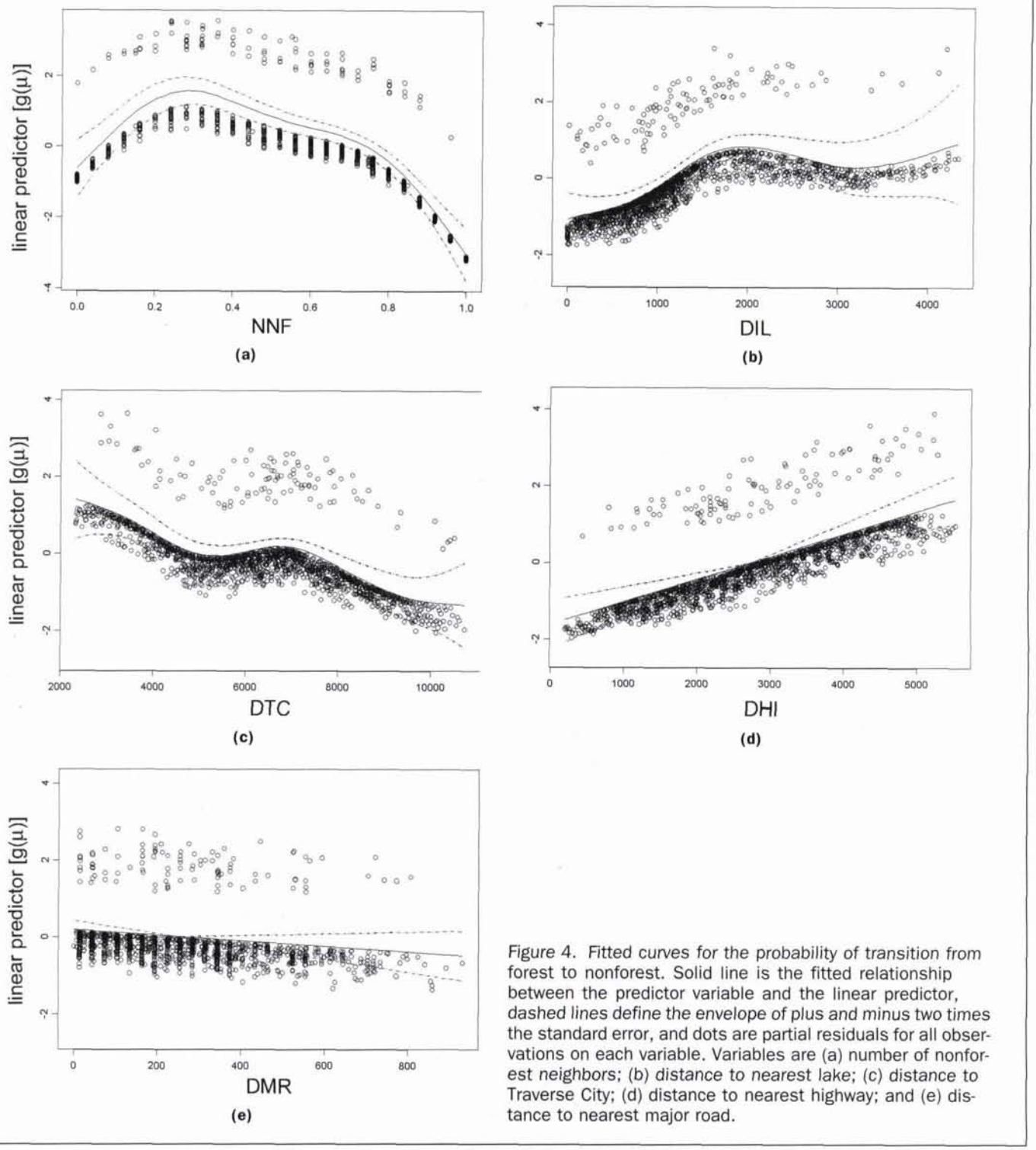

Figure 4. Fitted curves for the probability of transition from forest to nonforest. Solid line is the fitted relationship between the predictor variable and the linear predictor, dashed lines define the envelope of plus and minus two times the standard error, and dots are partial residuals for all observations on each variable. Variables are (a) number of nonforest neighbors; (b) distance to nearest lake; (c) distance to Traverse City; (d) distance to nearest highway; and (e) distance to nearest major road.

directions (Figure 6). The spatial pattern of transition probabilities is direction-independent (isotropic) and characterized by a small range of spatial correlation: 320 m for F to NF and 235 m for NF to F. However, the cross semivariogram displays a much longer range (1.6 km) in the north-south direction than in the east-west direction (800 m), which indicates that for a given separation distance two pixels are more likely to change land cover in opposite ways along the east-west direction. The spatial relationships between the two transition types observed in Figure 6 is consistent with the transition probability maps in Figure 5.

Simulation Results

One-hundred realizations of the 1985 LC map were generated using simulated annealing conditional to the transition probability maps of Figure 5 and the direct and cross semivariogram models of Figure 6 up to 480 m. Similar weights were assigned to the two components (Equations 9 and 10) of the objective

function. Because no node changed category after the 20th iteration, the simulation was stopped at iteration 20. The generation of an 88 by 160 LC map took 43 CPU seconds on a 1-GHz PC.

Figures 7a and 7b show realizations #1 and #2. The spatial patterns are reasonably close to the actual 1985 land-cover map of Figure 2, though with a few more isolated cells. All realizations displayed similar global proportions of F (30.31 to 30.33 percent) and NF (69.67 to 69.99 percent) pixels, which were very close to the actual proportions of 29.98 percent and 70.02 percent, respectively. The proportion of times F and NF are simulated over 100 realizations was computed for each pixel. The most likely LC and the corresponding frequency of occurrence were then mapped (Figures 7c and 7d, respectively). Zones of low frequencies (i.e., close to 0.5) indicate regions where the prediction of land cover is uncertain, which generally corresponds to borders between forest and nonforest zones in 1973.

The rank correlation coefficient between simulated and target transition probabilities was 0.638 for F to NF transition and 0.772 for NF to F transition, illustrating good performance of the simulation procedure. Figure 8 shows that the reproduction of spatial patterns of change is satisfactory over the distance of 480 m that was taken into account in the objective function. Imposing reproduction over larger distances would require using a large number of lags in the objective function (Equation 10), which would slow down the convergence of the algorithm.

Discussion and Conclusions

The generalized additive models (GAMs) of forest transition probabilities describe the spatial locations of forest-cover changes in the Traverse City study site during the 1980s. Variables describing location relative to existing forest, infrastructure, the market center, and surface water features were much more likely to have an influence on the models than were site variables describing the local terrain—none of which added significantly to either of the models. This suggests that spatial interaction with existing land cover and socioeconomic processes are the dominant drivers to forest-cover change over this relatively small area for this time period. Transition from NF to F was more common near existing forest, and the transition from F to NF was more likely on the borders of larger forest

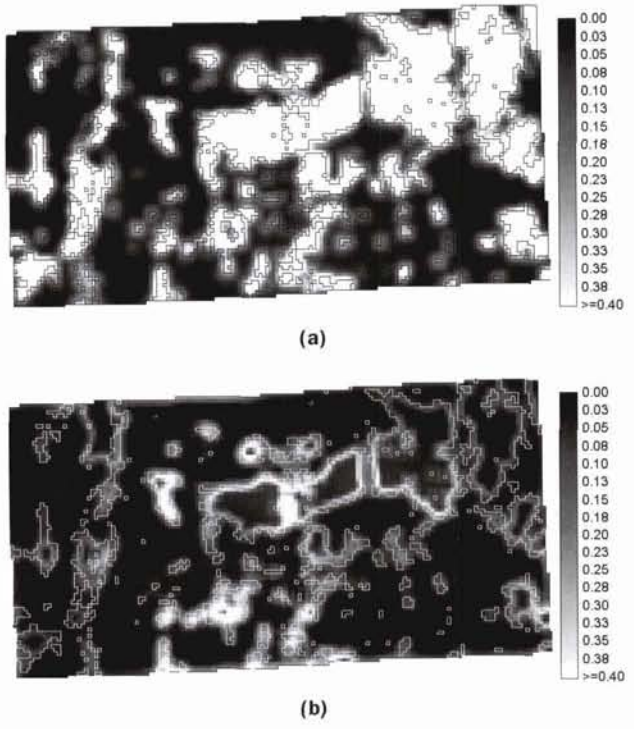

Figure 5. Transition probability maps predicted using calibrated generalized additive models (GAMs). (a) represents the probability of nonforested areas transitioning to forest; (b) represents the probability of forested areas transitioning to nonforest. Black (a) and white (b) lines are the forest patch boundaries in the initial map (i.e., 1973).

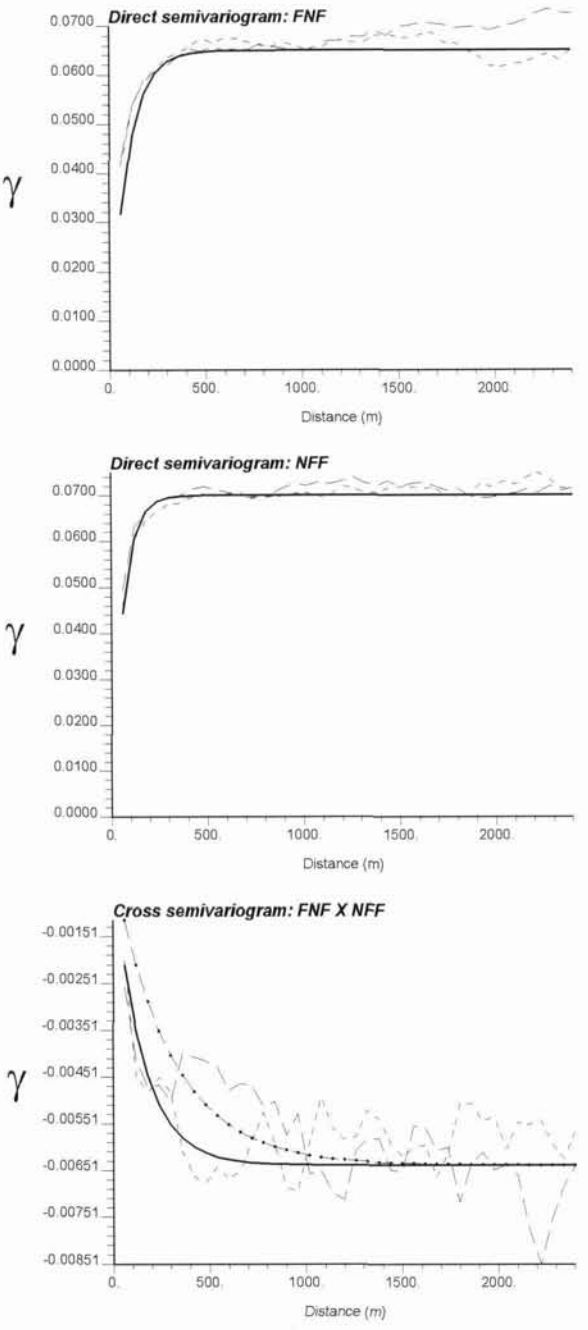

Figure 6. Experimental directional (——: NS, - - - - : EW) semivariograms and cross-semivariograms of indicators of changes, with the model fitted (solid line).

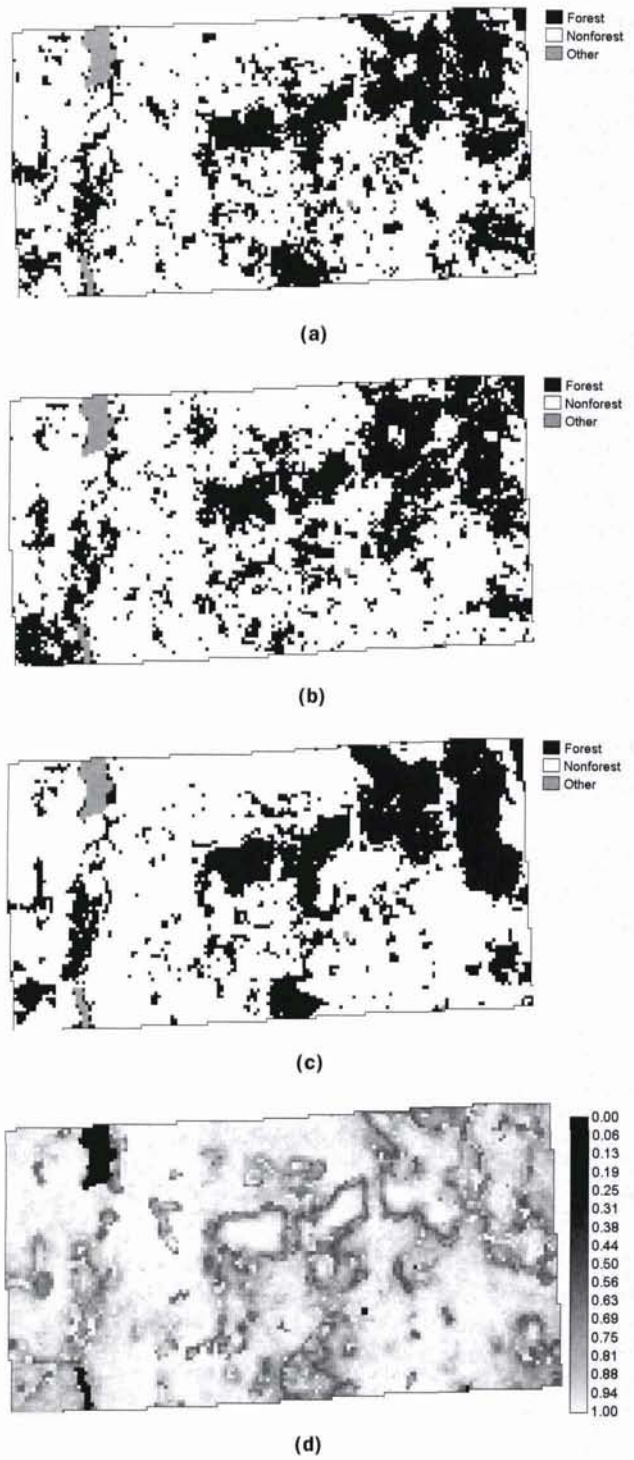

Figure 7. Two realizations of land-cover map for 1985 (a, b). The most likely land cover and the corresponding probability of occurrence, as estimated from 100 realizations, are mapped in (c) and (d), respectively.

patches, where there were relatively few nonforest neighbors in a 5 by 5 window, but more than about three. Location of roads had a strong influence on the spatial pattern of forest-cover dynamics in the study region. This is consistent with the location of the study area on the edge of a small but growing urban center. Not all roads, however, had the same effect on forest cover. Major roads depressed the NF to F transition over long distances, but residential streets affected the transition over shorter distances. Furthermore, nearness to highways tended to be positively related to forest regrowth and/or planting and negatively related to forest clearing. This may indicate that locations that were closer to the highways had already undergone

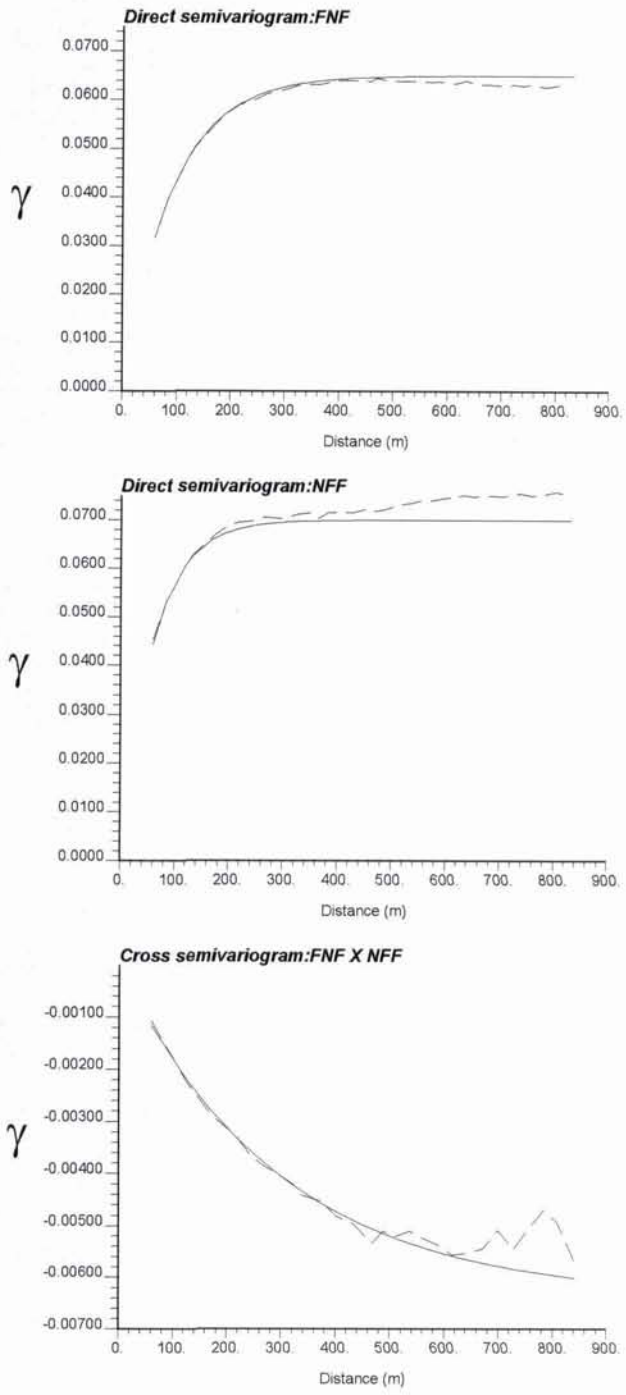

Figure 8. Experimental (cross) semivariograms of indicators of changes computed from the first realization, with the target models of Figure 6 (solid line). Distances for cross semivariogram values were rescaled so that anisotropic values plot on a single graph.

development and were less likely to be cleared during the study period.

First results indicate that the simulation algorithm presented here generates land-cover maps that reproduce reasonably well the spatial patterns of changes and the actual proportions of F and NF cells. The proportions of cells that change LC class are determined by the transition probabilities and the sill of the indicator semivariograms, both of which were modeled from the observed map pair. It is our intention to modify the simulation approach presented here to allow the user to input exogenous information about the rate of change and simulate the locations of the pre-specified number of changes on the basis of normalized transition probability maps and semivariograms. This modification will permit the incorporation of new predictions of the amount of landscape change derived from regional models of demographic and economic change (e.g., Hardie *et al.*, 2000). In this way the simulation can be coupled with regional-scale socioeconomic drivers of change, and its utility in socioeconomic scenario testing will be improved.

The method presented in this paper is very flexible and can be applied to the case of more than two landscape classes. For example, Goovaerts and Journel (1996) used a similar algorithm to simulate the spatial distribution of four rock types. Although the number of classes that could be jointly simulated is theoretically unlimited, it might become increasingly difficult to achieve a satisfactory reproduction of all the direct and cross indicator semivariograms for more than six to ten classes.

Stochastic simulation of land-cover change improves on deterministic or maximum-likelihood predictions because it can produce multiple realizations, all of which honor transition probability models and spatial patterns of change. The realizations (e.g., Figure 7, top) all give equally likely futures under the model specifications. Although the realizations can be summarized through maximum-likelihood estimation (e.g., Figure 7, bottom), analysis of future spatial patterns should focus on the realizations themselves. For example, to evaluate possible future forest fragmentation, one would calculate fragmentation statistics (e.g., McGarigal and Marks, 1995) on each realization to generate a distribution of values, which would describe the variability of forest fragmentation futures that are possible under the specified model.

Applying transition probability models and geostatistical descriptions to generate simulations of future landscape patterns requires one to assume some degree of temporal stationarity in the process (i.e., that the types of locations that change and patterns of change will be constant over time). Furthermore, applying the models generated in one place to another place would require the assumption of spatial stationarity. Because the stationarity assumptions are likely to be violated, it might be more useful to think of the simulation approach as a tool for scenario generation, as opposed to prediction in the strictest sense. An approach to applying the landscape simulation method presented here for scenario generation would be to generate multiple models of change from multiple study sites and/or multiple time periods. An example of the latter would be to use classified images for the same place but over many time periods. Four scenarios for future landscapes could be generated from this series of images, representing the combination of transition probability models from the periods of most and least rapid change and the geostatistical descriptions from the periods of most and least clustered change. These scenarios would present four extreme landscape situations that are all within the range of observed dynamics within the recent past (i.e., within the satellite record). Other scenarios could exploit differences in the spatial patterns of change among sites, districts, or regions.

The simulation approach assumes that the classifications and changes from which the spatial transition probability models, semivariograms, and initial map are derived are known with certainty. In fact, there is likely to be some degree of uncertainty (i.e., classification error) in these maps. Classification uncertainty could be easily incorporated into the procedure by using soft indicators (i.e., valued between 0 and 1) instead of hard or binary (0 or 1) indicators in the estimation of indicator variograms (Equations 6 and 7), as well as in the computation of probabilities of occurrence of the type given by Equation 8.

Iterative algorithms, such as simulated annealing, can become time-consuming as the size of the simulation grid increases. In this study, the convergence was facilitated by the use of non-conflicting and easy-to-update constraints in the objective function, as well as the systematic selection of the most favorable perturbation (MAP algorithm). This allowed the generation of multiple realizations within a reasonable amount of time. Further work will explore how the CPU time and convergence rate evolve as the size of the simulation grid increases, more landscape classes are added, and more constraints, such as reproduction of regional LC proportions, are imposed.

Acknowledgments

This work is supported by the Land-Cover and Land-Use Change (LCLUC) program of the National Aeronautics and Space Administration (NASA), under grant number NAG5-11271.

References

Baker, W.L., 1989. A review of models of landscape change, *Landscape Ecology*, 2:111–133.

Bell, E.J., 1974. Markov analysis of land use change—Application of stochastic processes to remotely sensed data, *Socio-Economic Planning Sciences*, 8(6):311–316.

Bockstael, N., 1996. Modeling economics and ecology: The importance of a social perspective, *American Journal of Agricultural Economics*, 78(5):1168–1180.

Brown, D.G., 1994. Predicting vegetation at treeline using topography and biophysical disturbance variables, *Journal of Vegetation Science*, 5(5):641–656.

Brown D.G., J.D. Duh, and S. Drzyzga, 2000a. Estimating error in an analysis of forest fragmentation change using North American Landscape Characterization (NALC) data, *Remote Sensing of Environment*, 71:106–117.

Brown D.G, B.C. Pijanowski, and J-D. Duh, 2000b. Modeling the relationships between land-use and land-cover on private lands in the Upper Midwest, *Journal of Environmental Management*, 59:247–263.

Burrough, P.A., and R.A. McDonnell, 1997. *Principles of Geographical Information Systems*, Oxford, New York, N.Y., 333 p.

Carle, S.F., and G.E. Fogg, 1996. Transition probability-based indicator geostatistics, *Mathematical Geology*, 28(4):453–476.

Carle, S.F., and G.E. Fogg, 1997. Modeling spatial variability with one and multidimensional continuous-lag Markov chains, *Mathematical Geology*, 29(7):891–918.

de Bruin, S., 2000. Prediction the areal extent of land-cover types using classified imagery and geostatistics, *Remote Sensing of Environment*, 74(3):387–396.

Goovaerts, P., 1997. *Geostatistics for Natural Resources Evaluation*, Oxford, New York, N.Y., 483 p.

Goovaerts, P., and A.G. Journel, 1996. Accounting for local probabilities in stochastic modeling of facies data, *Society of Petroleum Engineers Journal*, 1(1):21–29.

Hardie, I.W., P.J. Parks, P. Gottlieb, and D.N. Wear, 2000. Responsiveness of rural and urban land uses to land rent determinants in the U.S. South, *Land Economics*, 76(4):659.

Hastie, T., and R. Tibshirani, 1990. *Generalized Additive Models*, Chapman and Hall, London, United Kingdom, 335 p.

Kyriakidis, P.C., and J.L. Dungan, 2001. A geostatistical approach for mapping thematic classification accuracy and evaluating the impact of inaccurate spatial data on ecological model predictions, *Environmental and Ecological Statistics*, 8(4):311–330.

Landis, J., and M. Zhang, 1998. The second generation of the California urban futures model. Part 1: Model logic and theory, *Environment and Planning B-Planning & Design*, 25(5):657–666

Lunetta, R.S., J.G. Lyon, B. Guindon, and C.D. Elvidge, 1998. North American Landscape Characterization dataset development and data fusion issues, *Photogrammetric Engineering & Remote Sensing*, 64(8):821–829.

McGarigal, K., and B. J. Marks, 1995. FRAGSTATS: *Spatial Pattern Analysis Program for Quantifying Landscape Structure*, General Technical Report PNW-GTR-351, USDA Forest Service, Pacific Northwest Research Station, Portland, Oregon, 122 p.

Meyer, W.B., and B.L. Turner, 1994. *Changes in Land Use and Land Cover: A Global Perspective*, Cambridge University Press, New York, N.Y., 537 p.

Moeur, M., and R. Riemann-Hershey, 1999. Preserving spatial and attribute correlation in the interpolation of forest inventory data, *Spatial Accuracy Assessment: Land Information Uncertainty in Natural Resources* (K. Lowell and A. Jaton, editors), Ann Arbor Press, Chelsea, Michigan, pp. 419–430.

Muller, M.R., and J. Middleton, 1994. A Markov model of land-use change dynamics in the Niagara Region, Ontario, Canada, *Landscape Ecology*, 9(2):151–157.

Phillips, J.D., 1990. A saturation-based model of relative wetness for wetland identification, *Water Resources Bulletin*, 26(2):333–342.

Pijanowski, B.C., D.G. Brown, B. Shellito, and G. Manik, in press. Using neural nets and GIS to forecast land use changes: A land transformation model, *Computers, Environment, and Urban Systems*.

Polhill, J.G., N.M. Gotts, and A.N.R. Law, 2001. Imitative versus non-imitative strategies in a land use simulation, *Cybernetics and Systems*, 32(1–2):285–307.

Schneider, L.C., and R.G. Pontius, 2001. Modeling land-use change in the Ipswitch watershed, Massachusetts, USA, *Agriculture Ecosystems and Environment*, 85:83–94.

Turner, B.L., D. Skole, S. Sanderson, G. Fischer, L. Fresco, and R. Leemans, 1995. *Land-Use and Land-Cover Change Science/Research Plan*, International Geosphere-Biosphere Programme and International Human Dimensions Programme, Stockholm, Sweden and Geneva, Switzerland, 132 p.

Turner, M.G., 1987. Spatial simulation of landscape changes in Georgia: A comparison of three transition models, *Landscape Ecology*, 1:29–36.

Veldkamp, A., and L.O. Fresco, 1996. CLUE: A conceptual model to study the conversion of land use and its effects, *Ecological Modelling*, 85(2–3):253–270.

Wear, D.N., M.G. Turner, and R.J. Naiman, 1998. Land cover along an urban-rural gradient: Implications for water quality, *Ecological Applications*, 8(3):619–630.

Winkler, G., 1995. *Image Analysis, Random Fields, and Dynamic Monte Carlo Methods*, Springer-Verlag, Berlin, Germany, 324 p.